Empirical Modeling of a Rolling-Piston Compressor Heat Pump for Predictive Control in Low Lift Cooling

N.T. Gayeski, Ph.D.
Associate Member ASHRAE

T. Zakula
Student Member ASHRAE

P.R. Armstrong, Ph.D.
Member ASHRAE

L.K. Norford, Ph.D.
Member ASHRAE

ABSTRACT

Measured performance and empirical modeling of an inverter-driven variable capacity heat pump are developed for use in a predictive control algorithm to achieve energy-efficient low-lift heat pump operation. A 0.75 refrigeration ton heat pump with rolling-piston compressor was tested at 131 steady-state operating conditions spanning pressure ratios from 1.2 to 4.8. Compressor speed, condenser fan speed, condenser air inlet temperature and evaporator air inlet temperature were varied to map the performance of the heat pump over a broad range of conditions including very low compressor speeds and pressure ratios. Empirical, regression-based curve-fit models of the heat pump power consumption, cooling capacity, and coefficient of performance were identified that accurately represent heat pump performance over the full range of test conditions. This model can be incorporated into model-based predictive chiller control algorithms where compressor speed, condenser fan speed and evaporator fan (or chilled water pump) speed can be varied in an optimal way to achieve significant annual cooling system energy savings.

INTRODUCTION

Inverter-driven variable capacity air conditioners, heat pumps and chillers can provide energy-efficient cooling, particularly at part load capacity. Varying the capacity of vapor compression systems enables operation at lower pressure ratios, or low lift, which fundamentally improves the coefficient of performance of the system by reducing the required compressor work while providing a similar cooling effect per unit refrigerant mass flow rate. This is illustrated in Figure 1, which shows a conventional and a low lift vapor compression cycle for refrigerant R22. A cycle with a lower condensing temperature, higher evaporating temperature, and/or slower compressor speed, the low lift cycle, is shown to achieve a slightly greater cooling effect (the area below the evaporation process line) than the conventional cycle with much less compressor work (the area inside the cycle polygon).

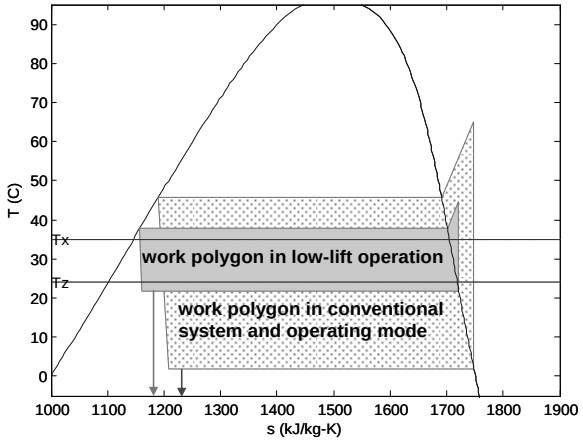

Figure 1. Low lift vapor compression cycle

Low lift operation of heat pumps and chillers in a cooling system can be achieved by employing radiant cooling, pre-cooling of thermal energy storage, and predictive control of compressor speed, condenser flow rate and evaporator flow rate (Armstrong et al 2009a, Armstrong et al 2009b) to meet daily cooling loads in a near-optimal manner. The combination of these strategies will here be called low lift cooling. Radiant cooling requires moderate chilled water temperatures, allowing for higher evaporating temperatures and pressures. Lower condensing temperatures, and thus lower condensing pressures, are achieved through nighttime operation of a heat pump or chiller to pre-cool thermal energy storage.

Predictive control of compressor speed, condenser flow rate, and evaporator flow rate allow the heat pump or chiller power consumption and coefficient of performance to be optimized over a 24-hour period to minimize energy consumption or operating cost. In order to achieve this optimal predictive control, a model of heat pump or chiller performance is necessary to map control variables and exogenous operating conditions to power consumption, cooling capacity and system coefficient of performance.

This paper reviews the status of heat pump and chiller performance empirical modeling, presents experimental results evaluating the performance of an air source heat pump with a rotary piston compressor particularly under low lift conditions, and presents empirical curve-fit models of the performance of the heat pump spanning a broad range of conditions.

LITERATURE REVIEW

Historically, heat pump and chiller cooling efficiency ratings focus on efficiency at a single design load, an average over seasonal conditions, or a small set of part-loads. These cooling efficiency ratings are represented by coefficient of performance (COP), seasonal energy efficiency ratio (SEER) for small air conditioners and heat pumps, and integrated part load value (IPLV) for large chillers. These are useful to engineers who are selecting efficient systems. However, at a given set of operating conditions the actual efficiency of a heat pump or chiller can be very different from these rated values. A more complete model of heat pump and chiller performance is necessary for model-based predictive control of compressor speed, condenser flow, and evaporator flow to achieve energy efficient low lift operation subject to different outdoor air temperatures, zone air or chilled water temperatures and cooling loads.

Existing models for heat pumps and chillers fall broadly into two categories, empirical models and physics-based models. Empirical models are typically regression-based polynomial curve-fit models of heat pump or chiller performance such as the DOE-2 chiller model (DOE 1980), but may also include neural networks and more advanced black-box modeling methods (Swider 2003). Physics-based models vary in complexity and degree of detail, but all apply fundamental physical principals to heat pumps, chillers, and their components to model system performance. Physics-based gray-box models such as the Gordon-Ng Universal Chiller Model (Gordon and Ng 2000) have parameters which can be identified from measured performance data for a given system, whereas white-box models use known engineering quantities to model performance.

Jin and Spitler (2002) and Sreedharan and Haves (2001) provide a broad review of heat pump and chiller models, focused primarily on steady-state chiller performance. Benapudi and Braun (2002) and Rasmussen (2005) review models of heat pumps and chillers suitable for model-based transient control optimization or to investiage new heat pump or chiller design options. The steady-state performance models are most appropriate for supervisory, predictive control applications necessary to achieve low-lift heat pump or chiller operation over a 24 hour look-ahead schedule (Armstrong et al 2009a, Armstrong et al 2009b).

Armstrong et al (2009a) developed a set of physics-based models for a variable speed compressor-chiller in a low-lift cooling application. Component models included a variable-speed reciprocating compressor, condenser and evaporator heat exchangers, an expansion valve, and a radiant cooling distribution system, valid down to low pressure ratios. The models can be used to predict chiller power consumption and COP for a given outdoor air temperature, zone air temperature, and cooling rate. Zakula (2010) extended the component modeling approach by including heat exchanger pressure drops, heat transfer coefficients that vary with flow rate, and inverter loss models, validated using data presented in this paper. Rather than use physics-based models, this paper focuses on empirical polynomial curve-fit modeling of heat pump and chiller performance suitable for use in a supervisory predictive control algorithm.

Empirical curve-fit models have been used extensively to represent steady-state heat pump and chiller performance. Stoecker and Jones (1982) presented an empirical bi-cubic curve-fit model of compressor power consumption as a function of refrigerant condensing temperature and evaporating temperature. This basic approach has been extended to create empirical multi-variable polynomial models of heat pump and chiller power consumption as a function of condenser fluid inlet (or outlet) temperature and evaporator fluid inlet (or outlet) temperature, as well as the cooling rate or part-load ratio, the ratio of cooling rate to reference cooling capacity at given set of conditions. The DOE-2 chiller model takes this approach to model chiller efficiency defined as electric input ratio (EIR), the reciprocal of COP, as a product of polynomials in chilled water supply temperature, condenser water return (or outdoor air) temperature, and cooling rate. The end result is a function that predicts power consumption as a product of two bi-quadratic polynomials in chilled water supply and condenser water supply temperatures and one quadratic polynomial in part-load ratio (Hydeman and Gillespie 2002). A bi-quadratic was used for optimal control purposes by Braun (1987).

Due to the increasing prevalence of chillers and heat pumps with variable speed compressors, and variable speed condenser and evaporator flow, researchers have begun to adapt multi-variable curve-fit models to these more efficient variable capacity systems. Hydeman and Gillespie (2002) noted that the existing DOE-2 chiller models have high error in power prediction, around 10 percent, for variable capacity chillers particularly at low loads and low condenser temperatures, i.e. low-lift conditions. They also note that the DOE-2 chiller model is inadequate for systems with variable condenser flow. Hydeman et al (2002) present a modified DOE-2 chiller model in the same format as the DOE-2 model but with condenser water return temperature as a variable instead of supply temperature. They also include temperature-dependent terms as well as third order terms in part-load ratio in the polynomial modifying chiller performance for part-load operation. They found that this modified DOE-2 chiller better represented centrifugal chillers with variable speed drives or variable condenser flow, but did not present data on chillers with both variable speed compressors and condenser flow. Armstrong (2009a) used a bicubic to fit ($r^2 = 0.9997$) the the modeled performance of a chiller-radiant cooling system with optimally-controlled compressor, chilled water pump and condenser fan speeds.

Another approach to empirical curve-fit modeling of variable-capacity heat pumps and chillers is to apply multi-variable polynomial functions directly to contolled variables, such as compressor speed or condenser fan speed. (Shao et al 2004) presented a curve-fit model of a variable speed compressor which predicts power consumption and refrigerant mass flow rate as a product of a typical bi-quadratic in evaporator and condensing temperature and a quadratic in compressor speed with a correction for actual suction temperature. Application of this model to three compressors showed the ability to predict compressor power, mass flowrate, and COP to within 4 percent or less average relative error for all three compressors. The same approach was applied by Aprea and Renno (2009) to predict cooling capacity for variable-speed reciprocating compressors. However, these approaches were not extended to model more than just compressor performance, i.e. a full heat pump or chiller.

Here we present an empirical curve-fit model for power consumption, cooling capacity, and EIR of a variable-capacity rolling-piston compressor heat pump as a quad-cubic function of compressor speed, condenser fan speed, outdoor air temperature and zone air temperature valid over a wide range of pressure ratio from 1.2 to 4.8. The model is useful in supervisory predictive control applications where compressor and condenser fan speeds can be optimized to achieve low-lift heat pump operation with radiant cooling and thermal storage. The performance a variable-capacity heat pump over the required wide range of conditions was carefully measured to develop and validate the empirical model.

EXPERIMENTAL MEASUREMENT OF VARIABLE CAPACITY HEAT PUMP PERFORMANCE

An experimental test stand was designed to test a small heat pump comprised of an outdoor unit compressor-condenser and a finned-tube indoor unit evaporator[1]. The outdoor unit contains a variable-speed rolling piston compressor with an accumulator, a finned-tube single-row condenser heat exchanger with a variable speed condenser fan, and an electronic expansion valve. The indoor unit contains a finned-

[1] Mitsubishi MUZ-A09NA outdoor unit and MSZ-A09NA indoor unit

tube double-row evaporator heat exchanger with a variable speed evaporator fan. The working refrigerant is R410A. A schematic of the system is shown in Figure 2 and a photo of the system in Figure 3. Only cooling performance was tested.

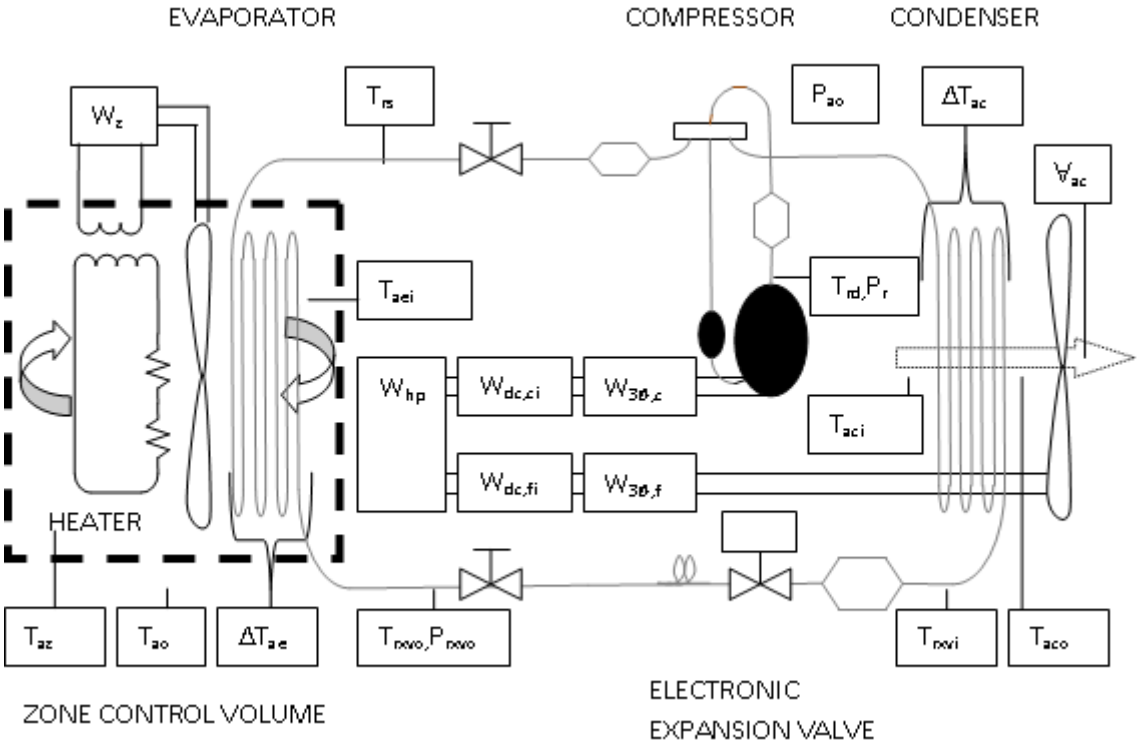

Figure 2. Heat pump test stand schematic and sensor locations

Table 1. Heat pump experimental test stand sensor descriptions

Label	Sensor description	Sensor type	Accuracy
T_{rs}	Suction refrigerant temperature	T-type thermocouple[2]	0.4%
T_{rd}	Discharge refrigerant temperature	T-type thermocouple	0.4%
T_{rxvi}	Expansion valve inlet refrigerant temperature	T-type thermocouple	0.4%
T_{rxvo}	Expansion valve outlet refrigerant temperature	T-type thermocouple	0.4%
T_{az}	Evaporator zone air temperature	T-type thermocouple	0.4%
T_{aei}	Evaporator inlet air temperature	T-type thermocouple	0.4%
T_{ao}	Ambient outside air temperature	T-type thermocouple	0.4%
ΔT_{ae}	Evaporator air temperature difference	9-junction thermopile with T-type thermocouples	0.4%
T_{aci}	Condenser inlet air temperature	T-type thermocouple	0.4%
T_{aco}	Condenser outlet air temperature	T-type thermocouple	0.4%
ΔT_{ac}	Condenser air temperature difference	9-junction thermopile with T-type thermocouples	0.4%
P_{rs}	Suction refrigerant pressure	Piezoresistive pressure transducer[3]	1%
P_{rd}	Discharge refrigerant pressure	Piezoresistive pressure transducer	1%
P_{rxvo}	Expansion valve outlet	Piezoresistive pressure transducer	1%
P_{ao}	Ambient air pressure measured at local weather station	Measured at weather station KMACAMBR9	
$\forall_{ac}$	Volumetric condenser air flowrate	Measured with anemometer traverse following ASHRAE Fundamentals (2005)	

[2] Omega PR-T-24-SLE T-type thermocouple with special limits of error
[3] Measurement Specialties MSP-300-XXX-P2-N1 pressure transducer

W_z	Total power to the zone control volume, including fan and heaters	Three phase analog power meter with separate current transducers[4]	0.5%
W_{unit}	Total power to the heat pump outdoor unit, including inverters, fan and compressor	Three phase analog power meter with separate current transducers	0.5%
$W_{dc,fi}$	DC power to the condenser fan inverter	Digital power meter[5]	0.1%
$W_{dc,ci}$	DC power to the compressor inverter	Digital power meter	0.1%
$W_{3\square,f}$	Three phase power from the inverter to the condenser fan	Digital power meter	0.1%
$W_{3\square,c}$	Three power from the inverter to the compressor	Digital power meter	0.1%

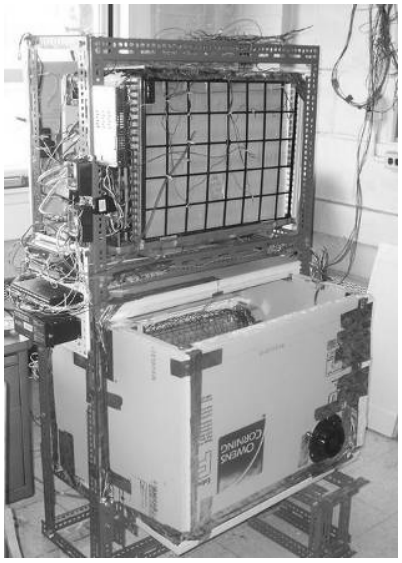

Figure 3. Heat pump test stand

As shown in Figure 3, the evaporator is contained in a sealed box made of extruded polystyrene foam insulation. This box represents a thermal zone being conditioned by the indoor unit. Air inside this box was recirculated through the evaporator by the evaporator fan, through a pair of electrical heaters serving as a thermal load, then back to the evaporator inlet. The evaporator box thus meets the requirements of a secondary fluid calorimeter (ASHRAE 2005).

Sensors were installed on the system to measure refrigerant temperatures and pressures, air temperatures, air temperature differences across the heat exchangers, electrical heater power providing load on the evaporator, fan power to the evaporator fan, total power to the outdoor unit, direct current (DC) power to the condenser fan and compressor inverters, and three phase power delivered to the condenser fan and compressor. The locations of these sensors are shown in Figure 2. Sensor descriptionsare given in Table 1.

The total thermal conductance across the evaporator box was measured to account for ambient heat gains which contribute to the cooling load in addition to the electrical heaters. To measure thermal conductance, the temperature difference between ambient conditions (or equivalently condenser air conditions) and air inside the insulated box was measured using thermocouples installed inside and outside of the box. A constant power was delivered to the heaters and fans inside the box to provide a constant heat rate. After a day of heating a steady-state temperature difference was observed, from which the total

[4] Wattnode WNB-3D-240-P analog power meter with Magnelab UCT current transducers
[5] Yokogawa WT-230 high frequency digital power meter

thermal conductance could be calculated. Repeated tests showed the conductance of the zone control volume, UA_z, was approximately 1.9 W/K (3.6 BTU/hr-F).

The volumetric airflow rate through the condenser was measured by traversing the condenser outlet air stream with a thermal anemometer. Samples of air velocity were taken at ten points along six radii following the methods for flow measurement outlined in ASHRAE Handbook of Fundamentals, Chapter 14 (ASHRAE 2005). Correlations between fan speed, airflow rate and fan power consumption were established in order to relate air flow rate to fan speed. The ambient air pressure during each test was recorded from weather station KMACAMBR9, and along with temperature, was used to calculate the density and specific heat of the condenser air.

Steady state performance data were collected at 131 chiller operating states spanning pressure ratios from 1.2 to 4.8, including combinations of the conditions listed in Table 2. The evaporator fan speed was fixed at the maximum speed. More generic testing could include varying the evaporator fan speed, however, evaporator fan speed was not varied for this research because the primary interest is in outdoor unit performance independently of the evaporator.

Table 2. Conditions for steady-state testing

Variable	Test conditions (combinations of the following)
Condenser air inlet temperature	15, 22.5, 30, 37.5, 45 °C (59, 72.5, 86, 99.5, 113 °F)
Evaporator air inlet temperature	14, 24, 34 °C (57.2, 75.2, 93.2 °F)
Compressor speed	19, 30, 60, 95 Hz
Condenser fan speed	300, 450, 600, 750, 900, 1050, 1200 RPM

Figure 4 shows, on the left, the outdoor unit EIR in terms of kW of electricity consumed (kW_e) per kW of cooling provided (kW_{th}) at the evaporator and its reciprocal, the COP, on the right, in both cases as a function of pressure ratio. The total heat pump "outdoor unit" COP, includes the power consumption due to electronics, the condenser fan inverter, the condenser fan, the compressor inverter, and the compressor which are all part of the heat pump outdoor unit. Evaluation of these quantities from the measured data listed in Table 1 proceeds as follows:

Outdoor unit EIR kW_e/kW_{th} = Total outdoor unit power consumpion / Evaporator cooling rate

(1) $$EIR_{unit} = 1/COP_{unit} = W_{unit} / \left(W_z + UA_z (T_{ao} - T_{az})\right)$$

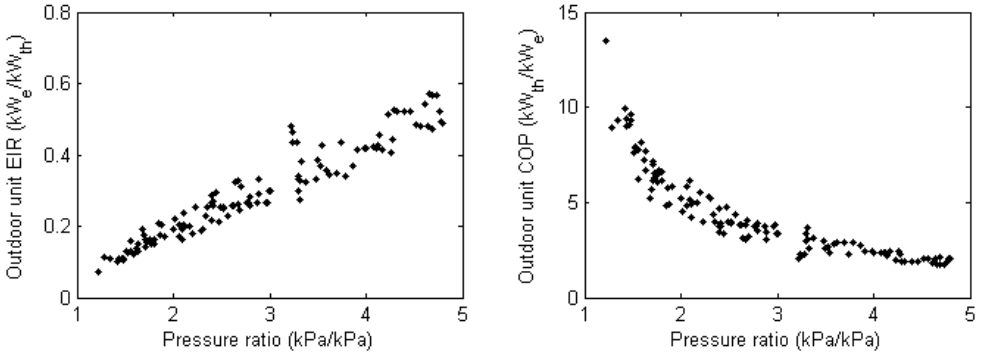

Figure 4. Outdoor unit efficiency, in EIR and COP

This view of the data shows how efficient the outdoor unit can be at low pressure ratios. At typical pressure ratios, above about 1.8 or 2, COPs range from three to four, but at lower pressure ratios the outdoor unit COP increases significantly from four to ten. The gains in the efficiency of the vapor compression cycle are somewhat offset by increased inverter losses at low speeds and increased fan power consumption. Inverter efficiency is in the range of 90 to 97 percent above ¼ load fraction dropping to 80%

under very light loads. Figure 5 shows the compressor inverter efficiency as a function of pressure ratio (with compressor speed noted) on the left and the condenser fan inverter efficiency as a function of air flow rate on the right. The high efficiency of todays power switching devices (inverters) over a broad range of speeds is an important enabling technology for high efficiency variable capacity heat pumps and chillers.

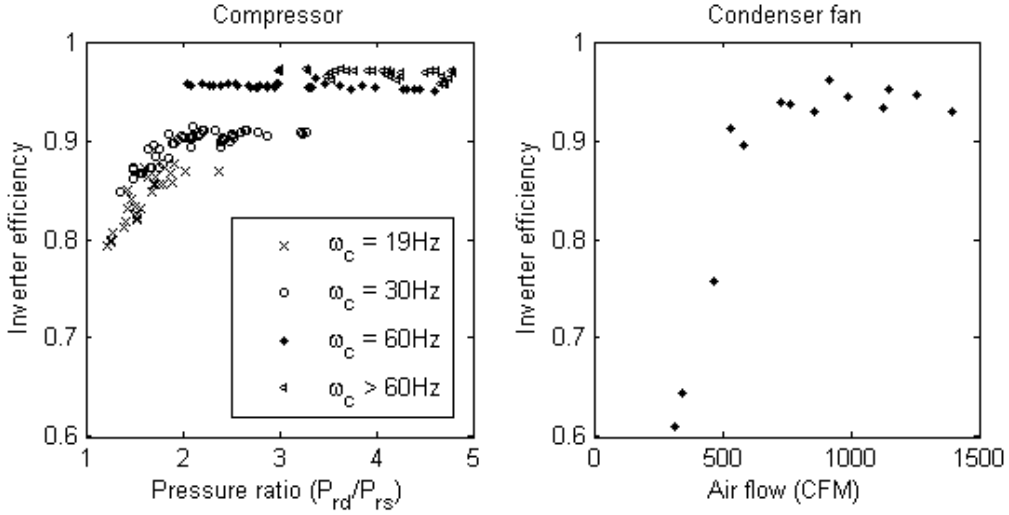

Figure 5. Inverter efficiencies

Energy and mass balances were performed on the heat pump performance data to validate the measurements at each steady state condition. These calculations use all of the measurements shown in Figure 2 except for W_{unit}, $W_{DC,fan}$ and $W_{DC,cmp}$. In a simple heat pump with zero piping and compressor jacket losses, the heat rejected at the condenser will equal the total heat absorbed at the evaporator plus the total work performed by the compressor on the refrigerant, or electrical power delivered to the compressor. The test stand includes measurements of condenser air volumetric flow, condenser air temperature difference, and condenser air pressure, from which to evaluate its specific heat and density. It also includes measurements of the three phase power delivered to the compressor and the cooling load on the evaporator. The cooling load on the evaporator includes both the electrical heater and evaporator fan power and the heat transfer into the zone control volume from the surrounding ambient conditions. With the foregoing measurements, a conservation of energy check can be applied to the three important heat and work transfers:

(2) Condenser heat load $$Q_{condenser} = \rho(P_{ao}, T_{aci}) c_p(P_{ao}, T_{aci}) \forall_{ac} \Delta T_{ac}$$

(3) Evaporator heat load $$Q_{evaporator} = W_z + UA_z(T_{ao} - T_{az})$$

(4) Compressor power $$W_{3\phi,c}$$

In the equations above, $\rho(P_{ao}, T_{ac})$ and $c_p(P_{ac}, T_{ac})$ are the pressure and temperature dependent ambient air density and specific heat.

The energy balance shown in Figure 6 shows good agreement between the condenser heat load and the evaporator heat load plus compressor power. The relative root mean square error (RMSE) across all measurements was 4.6 percent; the relatively higher errors are present particularly at low loads. The three phase power delivered to the compressor was used rather than total unit power or DC compressor power because the heat dissipated by the electronics, the inverters and the condenser fan does not interact with the vapor compression cycle. The compressor power was measured using a high frequency sampling digital power meter that accurately measures typical pulse-width modulated waveforms created by the inverters. The compressor and piping, apart from heat exchanger surfaces, were well insulated to minimize unmeasured heat transfers to or from the system.

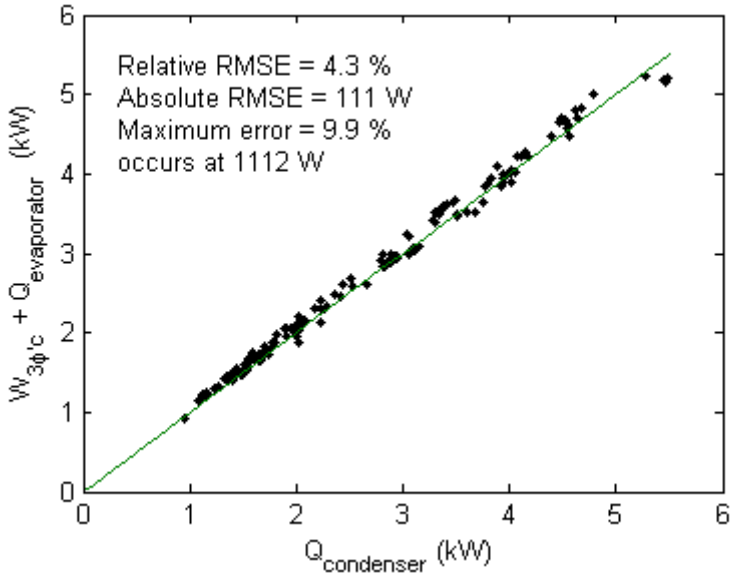

Figure 6. Data validation by energy balance

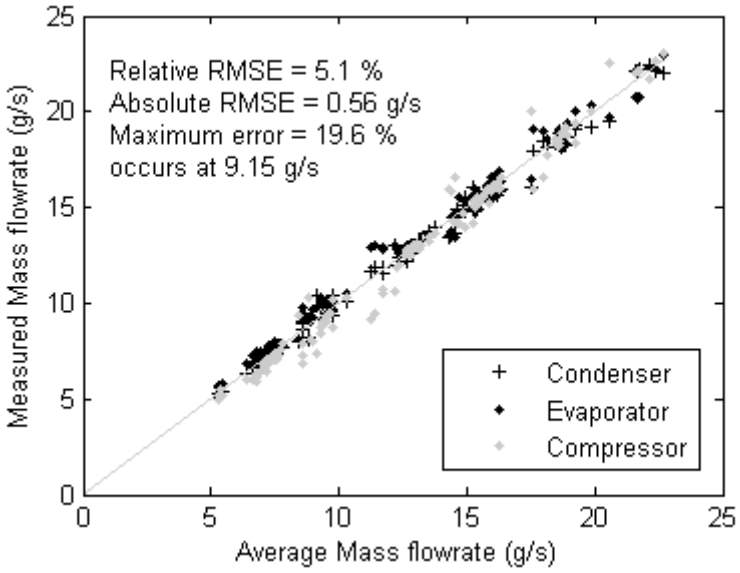

Figure 7. Data validation by mass balance

A mass balance was also performed to validate the pressure and temperature measurements used to evaluate refrigerant state (especially enthalpy and density) within the vapor compression cycle. The system is a single closed loop system and hence refrigerant mass flow rates must be the same through each component. Refrigerant mass flowrates through the compressor, condenser, and evaporator were calculated from measurements using the following equations:

(5) Compressor mass flowrate $\dot{m}_{compressor} = W_{3\phi,c} / \left(h(P_{rd}, T_{rd}) - h(P_{rs}, T_{rs})\right)$

(6) Condenser mass flowrate $\dot{m}_{condenser} = Q_{condenser} / \left(h(P_{rd}, T_{rd}) - h(P_{rd}, T_{rxvi})\right)$

(7) Evaporator mass flowrate $\dot{m}_{evaporator} = Q_{evaporator} / \left(h(P_{rs}, T_{rs}) - h(P_{rd}, T_{rxvi})\right)$

In the equations above, h is the pressure and temperature dependent refrigerant enthalpy for a given condition evaluated by REFPROP (NIST 2009) for R410A. The temperatures and pressures from which these enthalpies are calculated are listed in Table 1 and the compressor power and condenser and evaporator heat rates are calculated using Equations (2-4).

Two assumptions are implicit in the mass flow rate calculations. First, it is assumed that the discharge pressure is sufficient to calculate the enthalpy of the condensed liquid refrigerant exiting the condenser as an incompressible fluid. This is reasonable because in liquid state the refrigerant enthalpy is nearly independent of pressure. Second, it is assumed, because the expansion valve is well insulated, that the process of expansion through the electronic expansion valve is isenthalpic (adiabatic), and thus the enthalpy of the liquid refrigerant exiting the condenser is the same as the enthalpy of the two phase refrigerant entering the evaporator.

A comparison of these three calculated mass flow rates to the mean flowrate is shown in Figure 7. The relative RMSE for the mass flow rates is 5.1 percent with large errors at some low mass flow rate conditions. The compressor mass flow rate estimate was in error by as much as 19.5 percent at certain conditions. Errors result from jacket heat gain/loss, unknown circulationg oilfraction, and temperature and pressure measurement errors; all of these are exacerbated at low mass flow rate. Another complication is the oil mass fraction and circulation rate. The oil mass fraction is difficult to measure and was not measured on the test stand. As a result, the enthalpies calculated from pressure and temperature measurements, which assume the fluid is refrigerant R410A, may be in error due to the presence of oil mixed with the refrigerant (Willingham 2009). Equations (5-7) assume that the oil mass fraction is small enough that the change in refrigerant enthalpy completely dominates.

Overall, the test stand data show very reasonable agreement in energy balance and mass flowrates. These data have been used by (Zakula 2010) to develop improved physics-based heat pump component models for simulating low-lift compressor and chiller performance. The data will be used in the following section to develop empirical polynomial curve-fit models of heat pump performance.

EMPIRICAL MODELING OF VARIABLE CAPACITY HEAT PUMP PERFORMANCE

As discussed in the literature review, multi-variable polynomial curve-fits have long been used to represent the performance of heat pumps and chillers. Recently, these empirical models have been adapted to variable capacity chillers and heat pumps with inverter-driven variable speed compressors and variable speed condenser flow. A four-variable cubic polynomial was elected for modeling EIR, power consumption, and cooling capacity of the heat pump outdoor unit as a function of outdoor air temperature, zone air temperature, compressor speed and condenser fan speed.

One must be careful extrapolating polynomial models derived from experimental data outside the range of measured data. The data described above spans a wide range of condenser air inlet temperatures, evaporator air inlet temperatures, and compressor speeds but a more limited set of condenser fan speeds. This is the result of a deliberate choice to limit the number of test points due to the time required for each test; however the full range of the condenser fan speed at each tested compressor speed was exercised at four different combinations of outdoor air temperature and zone air temperature.

To account for this limited number of tested condenser fan speeds, a deliberately low (quadratic) dependence for the condenser fan speed variable was chosen. This dependence was observed for the pressure ratios and compressor speeds at which condenser fan speed was varied between 300 and 1200 RPM, and a similar dependence was assumed at other pressure ratios and compressor speeds. This quadratic dependence was enforced by eliminating high order cross terms in the fan variable, such as cubic terms in the condenser fan speed variable. The minima of these quadratics can vary with compressor speed, outdoor air temperature and indoor air temperature. The resulting curve-fit models have the following form:

$$DV = \begin{pmatrix} C_1 + C_2 T_{az} + C_3 T_{ao} + C_4 \omega_c + \\ C_5 T_{az}^2 + C_6 T_{ao}^2 + C_7 \omega_c^2 + C_8 T_{az} T_{ao} + C_9 T_{az} \omega_c + C_{10} T_{ao} \omega_c + \\ C_{11} T_{az}^3 + C_{12} T_{ao}^3 + C_{13} \omega_c^3 + \\ C_{14} T_{az}^2 T_{ao} + C_{15} T_{az}^2 \omega_c + C_{16} T_{ao}^2 T_{az} + C_{17} T_{ao}^2 \omega_c + \\ C_{18} \omega_c^2 T_{az} + C_{19} \omega_c^2 T_{ao} + C_{20} T_{az} T_{ao} \omega_c + \\ C_{21} f + C_{22} f^2 + C_{23} f T_{az} + C_{24} f T_{ao} + C_{25} f \omega_c \end{pmatrix} \quad (8)$$

In equation (8), DV, the dependent variable, can be either the cooling capacity Q, the whole unit power consumption P, or the EIR = 1/COP at a given outdoor air temperature T_{ao}, indoor zone air temperature T_{az}, compressor speed ω_c, and condenser fan speed f. The minima of the EIR across the condenser fan speed variable can be found by taking a partial derivative with respect to the fan speed. The optimal condenser fan speed as a function of outdoor air temperature, indoor air temperature, and compressor speed is given by the solution to equation (9), using the coefficients for the 1/COP curve.

$$C_{21} + 2C_{22} f + C_{23} T_{az} + C_{24} T_{ao} + C_{25} \omega_c = 0 \quad (9)$$

The resulting accuracies for this model choice are shown in Figure 8 over the full range of data tested, which spans a wide range of pressure ratios, outdoor temperature and indoor temperatures as described above. These graphs show that a multi-variable curve fit model can approximate the measured data well, with relative RMSE of 1.7, 5.5, and 4.7 percent for cooling capacity, power consumption, and EIR respectively. The most inaccurate model is the power consumption model, which has an absolute RMSE of 27 Watts. At low compressor speeds, low pressure ratios, and low power consumption this can lead to inaccuracy as high as 10-15 percent when the unit is consuming around 200 Watts. It may be possible to derive more accurate curve fit models or look up tables for cooling capacity, power consumption and EIR (or COP) as a function of the independent and controlled variables from physics-based modeling, e.g. (Zakula 2010).

The EIRs predicted from the curve fit models are shown in Figure 9. The graph on the left shows the EIR of the air conditioner outdoor unit as a function of compressor speed at a fixed condenser fan speed of 700 RPM. Within each graph are multiple curves representing the EIR at a given combination of indoor and outdoor temperatures, T_{az} and T_{ao}. For a given condenser fan and compressor speed, and with fixed evaporator fan speed, T_{az} and T_{ao} are surrogate parameters to the evaporating and condensing temperatures in the vapor compression cycle. The graph on the right shows the EIR of the outdoor unit as a function of condenser fan speed at a fixed compressor speed of 50 Hz.

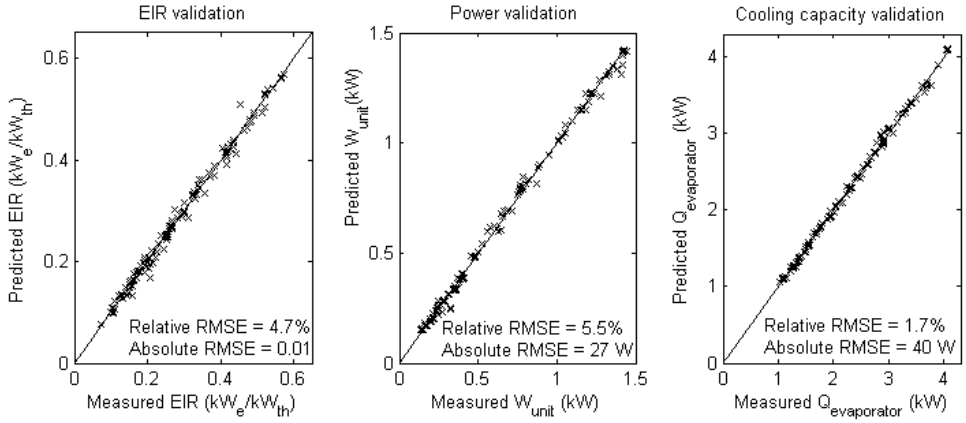

Figure 8. Accuracy of empirical polynomial curve-fit models

The performance curves can be used to predict power consumption, cooling rate and COP as a function of forecast outdoor temperature and desired internal zone temperature for given compressor and condenser fan speeds. Consequently, these curves can be incorporated into an predictive control algorithm in which compressor and condenser fan speeds are optimized to minimize energy consumption (or operating cost) subject to forecast outdoor conditions and desired zone temperatures. For buildings with significant thermal mass, pre-cooling can be performed to achieve low lift operation at night by finding a control sequence of optimal compressor and condenser fan speeds. This will be the subject of a future paper.

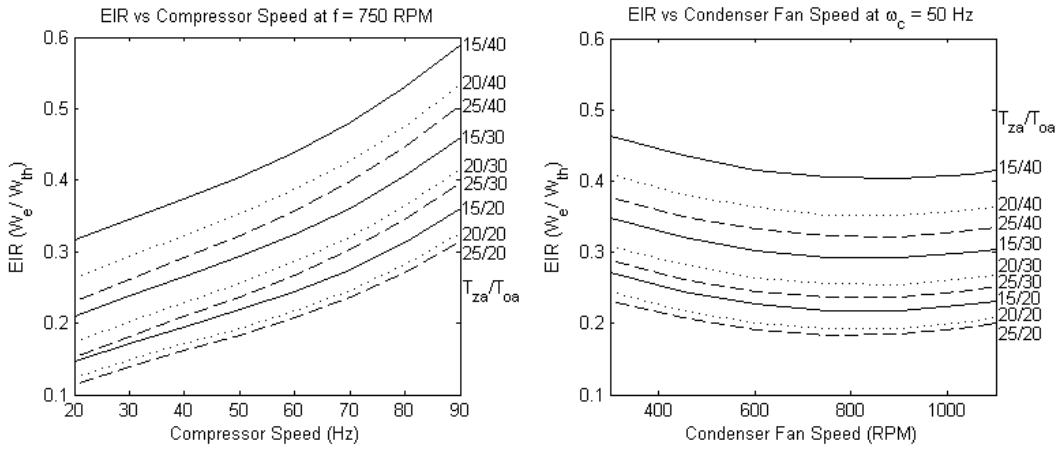

Figure 9. Empirical model heat pump performance (EIR) curves

SUMMARY AND DISCUSSION

An empirical curve-fit model of a vapor compression heat pump that is applicable over a wide range of pressure ratios, from 1.2 to 4.8, has been developed from detailed steady-state performance data of a rolling-piston compressor heat pump. Existing empirical models for heat pumps and chillers, such as the DOE-2 model, are inaccurate at low pressure ratios and for systems with variable speed condenser fans or compressors (Hydeman and Gillespie 2002). New curve-fit models were identified that are valid down to low pressure ratios over a wide range of variable speed compressor and condenser fan operation. Furthermore, these models explicitly include compressor speed and condenser fan speed as independent variables, making them well-suited for use in predictive control algorithms that optimize compressor and condenser fan speeds.

The curve-fit models are four-variable cubic polynomial functions for cooling capacity, power consumption, and EIR as a function of outdoor air temperature, zone air temperature, compressor speed and condenser fan speed. Quadratic dependence on condenser fan speed has been enforced by eliminating third order terms in condenser fan speed. The relative accuracy (in RMSE) of these models across the wide range of steady-state data are 1.7, 5.5, and 4.7 percent for cooling capacity, power consumption and EIR respectively for the rolling-piston compressor heat pump that was tested.

Creating similar quad-cubic models of other variable capacity heat pumps and chillers suitable for control applications can be accomplished in two ways. Physics-based models can be created that can be parameterized to accommodate different types and configurations of heat pumps and chillers (Zakula 2010). From these physics-based models, simplified quad-cubic curve-fits can be identified suitable for integration in predictive control algorithms. Alternatively, manufacturers may provide more detailed performance data for their products. Currently, manufacturers provide data primarily at test conditions established by AHRI standards. A standard for extended test conditions should be established. In the meantime manufacturers could provide detailed data on the capacity and COP of heat pumps and chillers

over a full range of compressor speed, condenser fan speed, evaporator fan speed and indoor and outdoor air temperatures. This would enable advanced heat pump and chiller control strategies such as predictive pre-cooling for load curtailment and efficient low-lift chiller operation.

The models presented here have been developed to support predictive control algorithms that optimize heat pump or chiller compressor and condenser fan speed over a 24-hour look-ahead period to efficiently meet cooling loads by pre-cooling thermal energy storage, such as a concrete-core radiant floor (Gayeski 2010). The framework for this predictive pre-cooling control has been established in prior research (Armstrong et al 2009a, Armstrong et al 2009b) and results from an experimental implementation of this pre-cooling control will be described in future papers.

ACKNOWLEDGEMENTS

The authors wish to acknowledge the Masdar Institute of Science and Technology for support of this research. The authors are also grateful for the support and advice of members of the Mitsubishi Electric Research Laboratory and the Pacific Northwest National Laboratory.

REFERENCES

Aprea, C. and C. Renno. 2009. Experimental Model of a Variable Capacity Compressor. *International Journal of Energy Research* 33:29-37.

Armstrong, P.R., W. Jiang, D. Winiarski, S. Katipamula, L.K. Norford, and R.A. Willingham. 2009a. Efficient Low-Lift Cooling with Radiant Distribution, Thermal Storage, and Variable-Speed Chiller Controls – Part I: Component and Subsystem Models. *HVAC&R Research* 15(2): 366-400.

Armstrong, P.R., W. Jiang, D. Winiarski, S. Katipamula, and L.K. Norford. 2009b. Efficient Low-Lift Cooling with Radiant Distribution, Thermal Storage, and Variable-Speed Chiller Controls – Part II: Annual Energy Use and Savings. *HVAC&R Research* 15(2): 402-432.

ASHRAE 1980. *ASHRAE Std. 41.2-1987 Standard Method for Airflow Measurement.*

ASHRAE. 2005. *ASHRAE Standard 41.9-2005, Calorimeter Test Methods of Mass Flow Measurements for Volatile Refrigerants*. Atlanta: American Society of Heating, Refrigerating and Air-conditioning Engineers, Inc.

ASHRAE. 2005. *ASHRAE Handbook – Fundamentals.* Atlanta: American Society of Heating, Refrigerating and Air-Conditioning Engineers, Inc.

Benapudi, S. and J. Braun. 2002. A Review of Literature on Dynamic Models of Vapor Compression Equipment. ASHRAE Research Project 1043-RP.

Braun, J.E., J.W. Mitchell, S.A. Klein, and W.A. Beckman. 1987. Performance and control characteristics of a large central cooling system. *ASHRAE Transactions* 93(1):1830-1852.

DOE 2 Reference Manual, Part 1, Version 2.1. Berkeley, California: Lawrence Berkeley National Laboratory.

Gayeski, N. 2010. *Predictive Pre-Cooling Control for Low-Lift Radiant Cooling using Building Thermal Mass*. Building Technology PhD dissertation. Massachusetts Institute of Technology.

Gordon, J., and K.C. Ng. 2000. *Cool Thermodynamics*. Cambridge International Science Publishing. United Kingdom.

Hydeman, M., N. Webb, P. Sreedharan, and S. Blanc. 2002. Development and Testing of a Reformulated Regression-Based Electric Chiller Model. *ASHRAE Transactions* 108(2)

Hydeman, M., and K. Gillespie. 2002. Tools and Techniques to Calibrate Electric Chiller Component Models. *ASHRAE Transactions* 108(2):

Jin, H., and J.D. Spitler. 2002. A Parameter Estimation Based Model of Water-to-Water Heat Pumps for Use in Energy Calculation Programs. *ASHRAE Transactions* 108(1)

NIST. 2009. NIST Reference Fluid Thermodynamic and Transport Properties Database (REFPROP): Version 8.0. NIST Standard Reference Database 23

Rasmussen, B.P. 2005. Dynamic Modeling and Advanced Control of Air Conditioning and Refrigeration Systems. PhD Dissertation. University of Illinois at Urbana-Champaign.

Shao, S., W. Shi, X. Li, and H. Chen. 2004. Performance representation of variable-speed compressor for inverter air conditioners based on experimental data. *International Journal of Refrigeration* 27(2004): 805-815.

Sreedharan, P., and P. Haves. 2001. Comparison of Chiller Models for Use in Model-Based Fault Detection. *Proceedings of the First International Conference for Enhanced Building Operations.* Austin, Texas. July 16-19, 2001.

Stoecker, W.S., and J.W. Jones. Refrigeration and Air Conditioning. USA: McGraw-Hill: 1982.

Swider, D.J. 2003. A comparison of empirically based steady-state models for vapor-compression liquid chillers. *Applied Thermal Engineering* 23(2003): 539-556.

Willingham, R.A. 2009. *Testing and Modeling of Compressors for Low-Lift Cooling Applications.* Master of Science in Mechanical Engineering thesis. Massachusetts Institute of Technology.

Zakula, T., N. Gayeski, L.K. Norford, and P.R. Armstrong. 2010. Heat Pump Simulation Model and Optimal Variable-Speed Control for a Wide Range of Cooling Conditions – Part I. (in preparation)